

NUMERICAL AND EXPERIMENTAL MODAL ANALYSIS OF FUEL-RODS

Shokoufeh Zargar¹, Ricardo A. Medina², Luis Ibarra³, and Justin Coleman⁴

¹ Ph.D. Student, Dept. of Civil and Environmental Engineering, University of New Hampshire, USA

² Associate Professor, Dept. of Civil and Environmental Engineering, University of New Hampshire, USA

³ Assistant professor, Dept. of Civil and Environmental Engineering, University of Utah, USA.

⁴ Seismic Engineer, Idaho National Laboratory, USA.

ABSTRACT

Numerical evaluation of the structural integrity of fuel assemblies requires reliable finite element models (FEMs) of fuel-rods. The focus of this paper is to experimentally validate the numerical model of spent nuclear fuel (SNF) rods exposed to vibrations during normal conditions of transport using quasi-static and modal testing. The numerical simulations are performed utilizing the finite element software Abaqus. For validation purposes, two different cases were studied: (i) fuel-rod without pellets (i.e. only cladding), (ii) fuel-rod with pellets in contact with one another where a gap exists between pellets and cladding. The fuel-rods used during the experiments were 1760 mm-long, which represents half of the length of a typical fuel-rod. Rods made of Zircaloy-4 and surrogate copper claddings with surrogate steel pellets were investigated. Impact hammer and shake table testing were conducted with the SNF rod supported at multiple points to identify natural frequencies. This paper incorporates the results from impact hammer testing only. Boundary conditions were designed to represent conditions similar to those experienced by the fuel-rod in a fuel assembly. Cases with missing supports representing damaged spacer grid were evaluated. Accelerations and deformations were used for validation of the FEMs. For fuel-rods with geometries, materials, and conditions consistent with those used in this study, it was concluded that the contribution of the steel surrogate pellets to the lateral stiffness of the fuel-rod is negligible. Furthermore, changes in boundary conditions (i.e., damaged spacer grids) caused variations in first-mode frequencies from 7 to 36 Hz.

INTRODUCTION

After several decades of on-site storage, spent nuclear fuel (SNF) will be transported to an interim storage facility or to a permanent disposal. However, the behavior and performance of fuel cladding and the structural elements of the fuel assemblies during normal conditions of transportation (NCT) after long-term storage is not well understood. If SNF rods degrade during extended storage, they could be susceptible to damage from vibration and impact loads during transport operations, releasing fission-product gases into the canister or the cask interior. An assessment of loss of structural integrity of the fuel assembly during transportation facilitates quantification of the associated risk. Due to uncertainties and lack of experimental data, numerical models of irradiated fuel-rods with appropriate boundary conditions are necessary for quantifying these risks (NWTRB, 2010).

A fuel assembly consists of a dozen or hundreds of fuel and control rods that are constrained at intermediate points by spacer grids. In this study, experimental and numerical simulations were conducted to preliminarily evaluate the dynamic properties of unirradiated fuel-rods under vibrational excitation. Numerical models were validated with results from experimental modal testing. Two different configurations were examined: (i) fuel-rod without pellets (i.e. only cladding), in which a copper cladding (C_u) was utilized as the physical specimen, and (ii) fuel-rod with pellets in contact with one another where a gap exists between pellets and cladding. In this latter case, Zircaloy-4 (Zr-4) and surrogate copper fuel-

rods were utilized. This study focuses on the quantification of the effect of boundary conditions and Pellet-Cladding Interaction (PCI) on the natural frequencies of vibration of unirradiated fuel-rods.

EXPERIMENTAL AND NUMERICAL MODAL ANALYSIS

Test Configurations and Material Properties

Fuel assemblies' types and configurations vary significantly. In this study, the distances between the spacer grids were adopted from a Westinghouse 17×17 (WE) optimized fuel assembly (OFA) pressurized water reactors (PWR): 632, 522, 522, 522, 522, 522, and 511 mm (DOE/RW-0184, 1987). The Zircaloy-4 rod used in this research was obtained from a previous experiment at Idaho National Laboratory. Its overall length is approximately 50% of the total length of a fuel-rod in a Westinghouse fuel assembly. The unsupported lengths used in the tests are 632, 522, and 522 mm (see Figure 1), which is consistent with sections with the largest spans in the original WE 17×17 OFA fuel assembly configuration. This approach will allow capturing lower modal frequencies that are consistent with the most dominant flexural modes of the full-length rod as compared to those obtained using constant spans of 522 mm.

The calibration of numerical models based on experimental results was conducted using four variations of the basic fuel-rod configuration illustrated in Figure 1. In this process, modal frequencies were identified for each of the cases described Table 1. These cases are a representative of different SNF rod support conditions. *Case I* represents undamaged spacer grids (Figure 1). *Cases II* and *III* consider that one of the interior spacer grids cannot provide adequate support due to previous damage (e.g., the development of gaps between a spacer grid and the SNF rod). Because spacer grids are not equally spaced along the length of the fuel-rod, each case provides different unsupported lengths. The configuration of *Case IV* is representative of significant gaps between both interior spacer grids and the fuel-rod. *Case IV* is also consistent with the condition of uplift of the fuel assembly within the basket (Adkins et al. 2013). All cases were evaluated for Zr-4 with surrogate steel pellets. The copper (C_u) cladding with and without surrogate steel pellets was investigated only for *Case IV*.

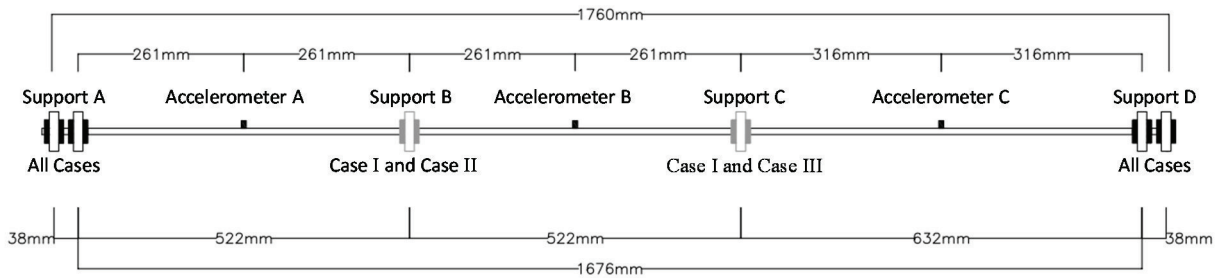


Figure 1. Location of supports and position of accelerometers for all test cases of the Zircaloy-4 rod

Table 1. Test cases

Cases	Number of spans	Spans length (mm)
I	three	522-522-632
II	two	522-1154
III	two	1044-632
IV	one	1676

The available Zircaloy-4 (Zr-4) cladding is a typical component of a PWR. The Zr-4 rod contains surrogate steel pellets that represents the uranium dioxide UO_2 pellets used in an actual fuel assembly and a plenum

spring. The dimensions of the Zr-4 fuel-rods and the surrogate steel pellets are presented in Table 2. The nominal material properties of the unirradiated Zr-4 (Matweb, 2015) and surrogate steel pellets were used in the finite element model (FEM). The dimensions and material properties of the C_u tube and the steel rod used for numerical validations were obtained from the supplier (Copper-Tube, 2015 and Steel-Rod, 2015). The gap sizes between the cladding and surrogate steel pellets are 0.08 and 0.12 mm for the Zr-4 and C_u cladding, respectively.

Table 2. Material properties and dimensions of fuel-rods and surrogate steel pellets

Characteristics	Zircaloy rod properties		Copper rod properties	
	Zr-4 cladding	Steel pellets	C_u cladding	Steel pellets
Outer Diameter (mm)	10.72	9.36	12.7	10.72
Inner Diameter (mm)	9.52	-	10.96	-
Length (mm)	1760	12.88	1760	12.88
Yield Strength (MPa)	381	640	207	640
Poisson Ratio	0.37	0.3	0.355	0.3
Modulus of Elasticity (MPa)	99,300	210,000	117,211	210,000
Nominal Density (ton/mm ³)	6.59 E-9	7.83 E-9	8.94 E-9	7.83 E-9

Modal Testing

Modal testing of fuel-rods was performed at the University of New Hampshire (UNH) Structural Laboratory with an impact hammer (modal Hammer), as well as a shake table. For the shake table cases, a single square wave support excitation was applied. Consistent results were obtained between these two approaches and results reported herein are for impact-hammer testing. By positioning several accelerometers through the length of the fuel-rod and imposing an impact at different locations, the fuel-rod was excited and the accelerations were recorded. Three accelerometers with an acceleration range of ± 500 g and a unit weight of 1.7 grams were located on the fuel-rod at attachment points corresponding to the mid-spans of the fuel-rod configuration of *Case I* defined as accelerometers “A”, “B” and “C” in Figure 1. These accelerometers were selected because of their small weight and high acceleration range. The acceleration was measured with a sampling rate of 2,560 samples per second. The measured vibration response of the structure was transformed into frequency response function using the Fast Fourier Transformation (FFT) algorithm. Figure 2 illustrates (a) the acceleration time history and (b) the corresponding FFT of acceleration measured by different accelerometers along the length of the Zr-4 cladding with surrogate steel pellets (*Case IV*). The peaks in Figure 2(b) show that the accelerometers are capturing the fundamental lower frequencies of the fuel-rod, which are identified by vertical grey lines.

Numerical Models

The cladding and the surrogate steel pellets with their interface gaps (0.08 and 0.12 mm for Zr-4 and C_u fuel-rods, respectively) were modelled in three dimensions using Abaqus (ABAQUS, 2013). The cross section mesh shown in Figure 3 was generated with C3D8R elements (solid reduced integration linear brick elements) for the surrogate steel pellets, and C3D8I elements (An 8-node linear brick, incompatible modes) for the cladding. As observed in the figure, the surrogate steel pellets were sitting at the bottom of the cladding (Zr-4 and C_u) in the model. When the rod is horizontal, gravity will cause the bottom of the pellets to be initially in contact with the cladding. General contact was assigned for all contacts in the numerical model. In linear perturbation analysis (i.e. modal analysis) in Abaqus, contact conditions at the beginning of the analysis are maintained. At the locations of the supports, reference points (RP) were located at the center of the cladding. Using the coupling constraint in Abaqus, the reference points were connected to the cladding and the boundary conditions were imposed on the RP. All supports were restrained against

displacement in the transverse (X), vertical (Y) and longitudinal (Z) axes and rotation about the longitudinal (Z) axes, since the cladding in the experiment was not allowed to displace or twist at the supports. Impact forces were applied in the transverse direction rod (X-direction in Figure 3), i.e., orthogonal to the centroidal axis of the fuel-rod. In this paper, only the natural frequencies in the transverse direction are reported.

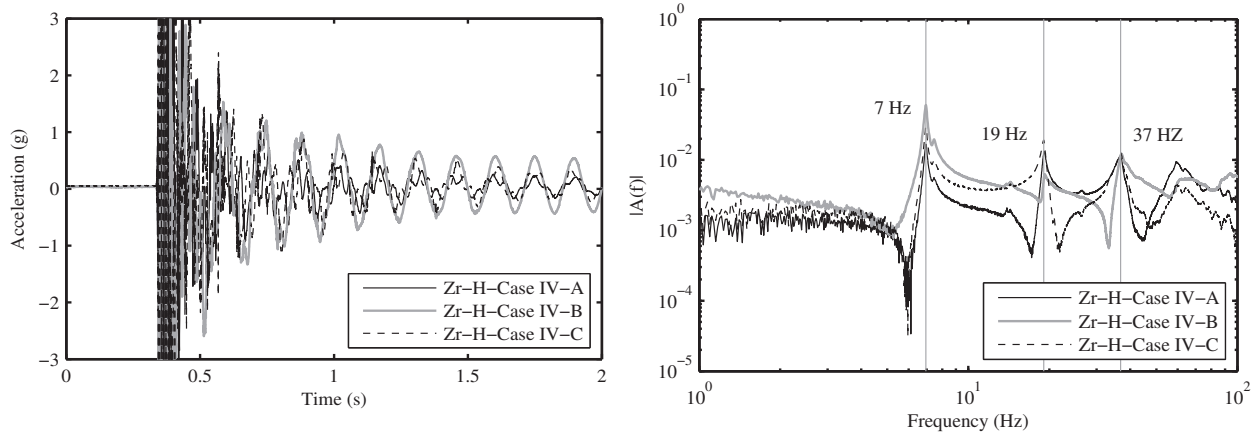


Figure 2. (a) Acceleration time history and (b) FFT response of the accelerometers “A”, “B” and “C” mounted on the Zircaloy-4 cladding with surrogate steel pellets for *Case IV*

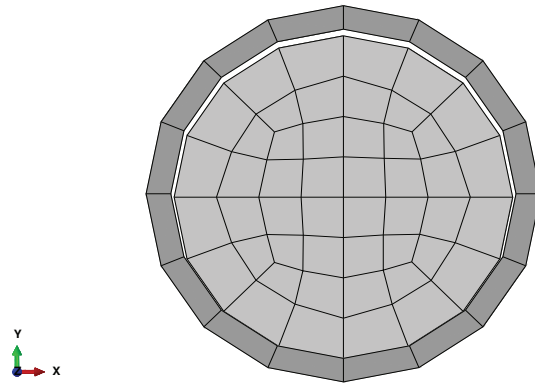


Figure 3. Typical cross-section mesh configuration of the fuel-rod and surrogate pellets

Analysis and Results

The available Zr-4 cladding specimen with surrogate steel pellets is sealed at both ends, and it was not open for the vibration tests to prevent damage to the Zr-4 material. Therefore, the Zr-4 rod without pellets was not tested. On the other hand, the C_u cladding was used to perform the experiments with and without surrogate steel pellets to capture the contribution of the steel pellets to the modal frequencies of the rod and attempt to isolate this effect from that of changing boundary conditions. The C_u cladding (without surrogate steel pellets) attached to the UNH shake table is shown in Figure 1.

Impact tests were performed to excite the C_u rod and record acceleration responses at the locations A, B, and C shown in Figure 1. At first, support conditions were imposed on the experimental specimen via a single clamp at each end (Figure 5). The first three experimental and numerical modal frequencies were calculated and tabulated in Table 3 based on various assumptions in the numerical model. A numerical model with pin supports at the end of the rod resulted in frequencies that are within 12% of those identified

experimentally. Thus, using one clamp was equivalent to having pinned supports. Subsequently, two clamps were used at the ends and the experiment was repeated. The numerical modal analysis for a fixed support condition exhibited higher frequencies than those obtained experimentally as shown in Table 4. An updated numerical model was calibrated to capture the modal response of the experiment for the case with dual clamps. Spring elements with a rotational stiffness of 800 N.m/rad about the transverse (X) and vertical (Y) axes were incorporated in addition to the pin-end supports to represent the finite rigidity provided by the dual clamps and more accurately capture the modal frequencies of the test configuration. Differences in the first three modal frequencies between the numerical model and the experiment reduced to less than 1%.

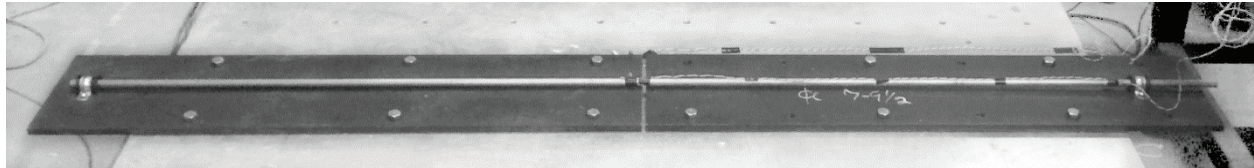


Figure 4. Copper cladding (without surrogate steel pellets) with a single clamp at each end

Figure 5. One- and two-clamps end support configurations

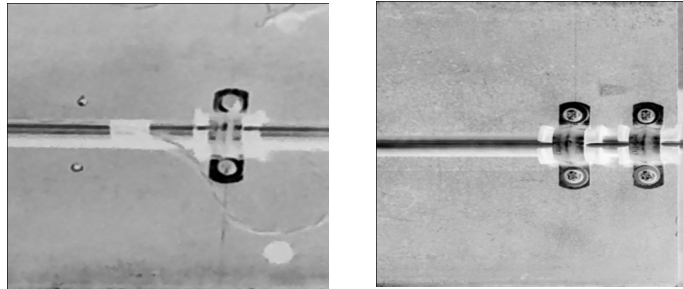


Table 3. Experimental and numerical natural frequencies of C_u cladding without pellets considering a single clamp at end supports

Mode	Frequency		
	Experimental	Numerical "Pinned-end supports"	
		Hz	Hz
1	10.8	8.5	21
2	37.5	33.9	10
3	80.8	75.7	6

Table 4. Experimental and numerical natural frequencies of C_u cladding without pellets considering dual clamps at end supports

Mode	Frequency				
	Experimental	Numerical "Fixed-end supports"		Numerical "Semi-rigid-end supports"	
		Hz	Hz	Error (%)	Hz
1	16.2	19.4	-20	16.7	-3
2	46.8	53.3	-14	46.6	1
3	92.7	104.4	-13	92.3	1

Experiments on Cu cladding with and without surrogate steel pellets, as well as Zr-4 cladding with surrogate steel pellets, were performed to measure the contribution of the surrogate steel pellets to the bending stiffness of the rod. For each experiment, a single span (1,676 mm, *Case IV*) simply supported member was loaded quasi-statically with a concentrated load at the mid-span. The supports were considered rollers to eliminate any rotational stiffness at the supports. Deflections at the mid-span were measured using a digital-image correlation system (DIC). Figure 6, illustrates the ratio of the measured experimental deflection of the Cu cladding (Cu, hollow circles) without pellets, Cu cladding with surrogate steel pellets (Cu&St, hollow squares), and Zr-4 cladding with surrogate steel pellets (Zr&St, hollow triangles) to the calculated (numerical) deflection considering the stiffness of the cladding only. The difference between the average ratio (filled circle and filled square) for the Cu cladding with and without surrogate steel pellets was less than 1%. Table 5, shows that the natural frequencies from the numerical calibration of the Cu cladding with surrogate steel pellets model without considering the bending stiffness (EI) of the pellets (semi-rigid end support case, considering pin supports with rotational springs of 800 N.m/rad) are within 7% of the frequencies obtained from the experiment. The negligible bending stiffness contribution of the pellets is a consequence of the pellets boundary condition at the end of the cladding and the gap between the pellets and the cladding. In the Cu rod experiments, the ends of the cladding are covered with tape to prevent the pellets to move out. In the Zr-4 rod specimen, the plenum spring exerts an axial force on the pellets that minimizes the movement of the fuel pellets inside the fuel-rod during handling and transportation. For the Zr-4 cladding with surrogate steel pellets, the average ratio in Figure 6 demonstrates that deflections are within 8% of one another when the bending stiffness of the pellets is neglected. The plenum spring induces a slight increase in the bending stiffness of the rod, which has been neglected in this study. Similar results and conclusions were obtained when a smaller span length was used.

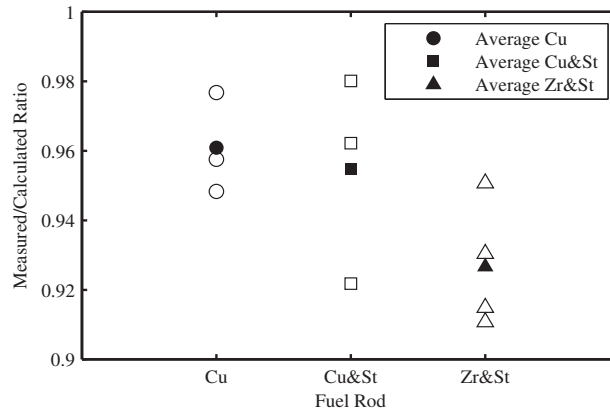


Figure 6. Ratio of measured to calculated displacement from individual quasi-static tests of Cu cladding without pellets (Cu, hollow circles), Cu cladding with surrogate steel pellets (Cu&St, hollow squares), Zr-4 cladding with surrogate steel pellets (Zr&St, hollow triangles), and their averages (filled shapes)

Table 5. Experimental and numerical natural frequencies for Cu cladding with surrogate steel pellets neglecting the contribution of bending stiffness of steel pellets considering dual clamps at end supports

Mode	Frequency				
	Experimental	Numerical "Fixed-end supports"		Numerical "Semi-rigid-end supports"	
		Hz	Hz	Error (%)	Hz
1	8.59	10.3	-20	8.91	-4
2	22.3	28.4	-27	24.89	-12
3	46.8	55.5	-19	49.33	-5

From here on, the discussion will focus only on the Zr-4 cladding with surrogate steel pellets. In all cases, dual clamps are used as end supports and single clamps as interior supports. The dual clamps were used to increase the frequency level of the rod. This implies that interior supports act as pin supports.

Case I

The span lengths in *Case I* are 522, 522 and 632 mm, which are consistent with the longer span lengths of WE 17 × 17 OFA fuel assembly. Experimental and numerical modal analyses were performed on the Zr-4 cladding with surrogate steel pellets. The effective modal mass of the first three natural frequencies of the fuel-rod are reported in the direction of the modal testing (X-direction in Figure 3) in Table 6. Furthermore, these frequencies fall within the frequency range from 2 to 50 Hz, which is consistent with the dominant excitation frequencies corresponding to the expected dynamic loading on fuel assemblies transported by rail (Adkins et al. 2013). In the numerical modal analysis the bending stiffness of the pellets was neglected based on the quasi-static bending tests conducted with the surrogate C_u and Zr-4 rods. However, the mass of the surrogate steel pellets was accounted for in the numerical model by imposing a uniform distributed mass along the length of the rod.

. Models with pin supports at the ends of the rod were also developed. In order to account for the support rotational resistance in these latter models, rotational springs were added to the pin supports. Spring elements with a uniform rotational stiffness about the transverse (X) and vertical (Y) axes were utilized. Rotational stiffness values were estimated by modifying the value obtained from the C_u cladding without surrogate steel pellets. The stiffness of the calibrated rotational spring for the C_u cladding ($(K_{\theta})_{Cu} = 800$ N.m/rad) was scaled based on the ratio of cross-sectional bending stiffness of the Zr-4 and C_u claddings, Equation 1. In this equation, E_{Cu} and E_{Zr} are the modulus of elasticity of C_u and Zr-4 claddings, respectively. Furthermore, I_{Cu} and I_{Zr} are the moment of inertia of C_u and Zr-4 claddings, respectively. A resulting rotational stiffness ($(K_{\theta})_{Zr}$) of 290 N.m/rad was calculated and used at end-support points for the numerical models of Zr-4 with surrogate steel pellets. The modal frequencies of the experiment and the calibrated model with semi-rigid end support connections were on average within 3% of the experimental modal frequencies for the first three modes as seen in Table 7. The corresponding numerical mode shapes for the first three modes are shown in Figure 8.

$$(K_{\theta})_{Zr} = \frac{(E_{Zr}I_{Zr})}{(E_{Cu}I_{Cu})} (K_{\theta})_{Cu} \quad (1)$$

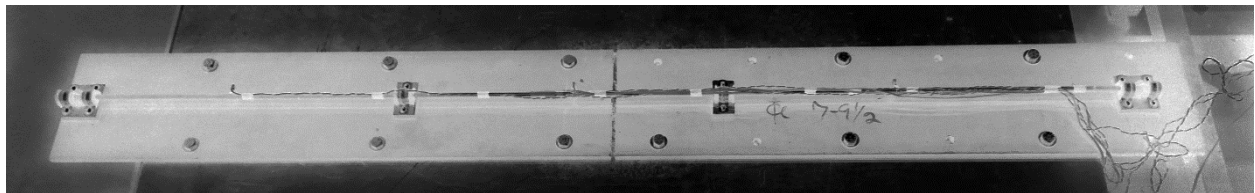


Figure 7. *Case I*, Zr-4 rod with surrogate steel pellets with dual clamps at each end support and a single clamp for the interior supports

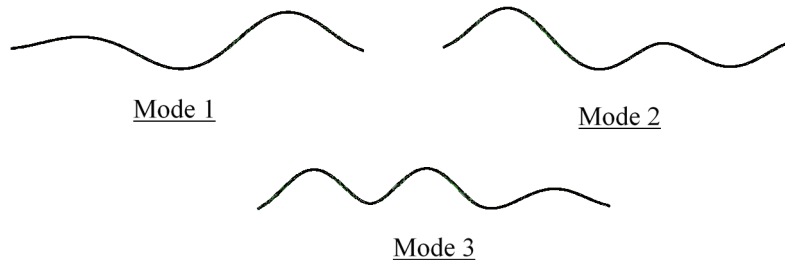


Figure 8. First three numerical mode shapes for *Case I*

Table 6. Modal effective mass ratio for Zr-4 cladding with surrogate steel pellets, *Case I*

Mode	Modal effective mass ratio
1	10.3
2	2.25
3	53.7

Table 7. Experimental and numerical natural frequencies of all cases for Zr-4 cladding with surrogate steel pellets considering dual clamps at end supports

Case	Mode	Frequency				
		Experimental Hz	Numerical “Fixed-end supports”		Numerical “Semi-rigid-end supports”	
			Hz	Hz	Error (%)	Hz
I	1	35.9	38.5	-7	34.4	4
	2	48.2	53.9	-12	47.9	1
	3	64.8	73.7	-14	66.6	-3
II	1	13.0	13.9	-7	12.5	4
	2	36.1	38.7	-7	35.1	3
	3	54.2	63.6	-17	54.9	-1
III	1	15.8	16.4	-4	14.6	7
	2	36.3	40.5	-12	35.4	2
	3	47.6	53.9	-13	48.2	-1
IV	1	6.99	7.64	-9	6.58	6
	2	19.3	21.0	-9	18.4	5
	3	36.8	41.2	-12	36.6	1

Case II

This case represents a condition in which one of the interior spacer grid springs experiences previous significant damage. Thus, a relatively large gap is assumed to exist between the fuel-rod and the damaged spacer grid springs or relaxation of the springs, which warrants neglecting the damaged support from the analysis. The resulting distances between undamaged spacers are 522 and 1,154 mm. To represent this condition, an interior support was removed at the desired location (*Support C* in Figure 1). The frequencies of the experimental modal test and numerical model with neglecting the contribution of the bending stiffness of the surrogate steel pellets are on average within 11% of one another when fixed-end supports are assumed (Table 7). By calibrating the end supports, as described above (i.e., modelling them as pin supports with rotational springs) the average percentage difference between experimental and numerical modal frequencies decreases to 3% (Table 7). The loss of an interior spacer grid causes a significant reduction in the first three modal frequencies of the rod, which would make it more prone to damage under normal conditions of transport when dynamic input motions are dominated by lower frequencies.

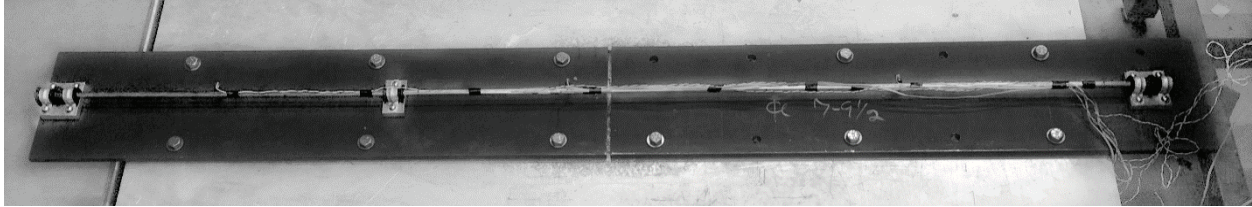


Figure 9. *Case II*, Zr-4 rod with surrogate steel pellets with dual clamps at each end support and a single clamp for the interior support

Case III

This case is similar to *Case II* except that *Support B* is removed as opposed to *Support C* (see Figure 1). The distances between the undamaged spacers are now 1,044 and 632 mm. The first-mode frequency of the Zr-4 rod with surrogate steel pellets increases (Table 7), as the longer span of *Case III* is shorter than the longer span of *Case II*. The same calibration factors used for *Case II* were implemented on the numerical model of *Case III*. The resulting first three numerical modal frequencies differ on average by less than 4% with respect to the experimental modal frequencies. This experiment highlights the sensitivity of the location of the damaged spacer grids on the resulting first-mode frequency of a fuel-rod.

Case IV

This configuration is representative of damage to all interior spacer grids, which would generate gaps between the spacer grid wall and the fuel-rod. Alternatively, this case could be used to represent possibility of uplift of the interior supports of the entire assembly within the basket due to vertical vibration or shocks during transportation (Adkins et al. 2013). For a typical fuel assembly the first mode frequency can be estimated roughly in the range of 3 to 6 Hz (Klymyshyn et al. 2013). Based on previous numerical models of fuel assemblies (Adkins et al. 2013), the first and the second flexural modes for the full fuel assembly considering various values of flexural rigidity (stiffness) for the fuel-rod are estimated about 5 and 10 Hz, respectively. Because the length of the Zr-4 rod used in this study (1,760 mm) is approximately equal to 50% of the active length of a rod in a WE 17 × 17 OFA assembly is 3,602 mm (the overall length is about 3,860 mm), the first-mode frequency of *Case IV* should be close to the second-mode frequency of the full fuel assembly. The resulting modal frequencies are shown in Table 7. The same calibration process applied to the previous three cases on the exterior supports was applied to this case. Likewise, the contribution of the surrogate steel pellets to the bending stiffness of the fuel-rod was also neglected. The resulting numerical modal frequencies had on average 4% difference with respect to the frequencies obtained from experimental modal testing.

CONCLUSIONS

An experimental modal analysis by utilizing an impact hammer was performed on fuel-rods to investigate the dynamic properties of an intact Zr-4 fuel-rod with surrogate steel pellets. The test results were used to validate numerical models of the fuel-rod. Fuel-rods with two, three, and four support points were investigated to quantify the effect of (i) the bending stiffness of pellets, and (ii) damage to support conditions (used herein to represent spacer grids) on the modal frequencies of a linear elastic fuel-rod. The numerical models accounted for contact between surrogate steel pellets, as well as between the pellets and the cladding. Because an intact rod was used, bonding between pellets and cladding was neglected.

The contribution of the surrogate steel pellets to the bending stiffness of the fuel-rod was negligible for: (i) the Zircaloy-4 cladding with surrogate steel pellets with a uniform gap between them of 0.08 mm, and (ii) the copper cladding with surrogate steel pellets with a uniform gap between them of 0.12 mm. This observation is not consistent with other studies in which a small percentage (e.g., 10%) of the bending

stiffness of the pellets is accounted for in the numerical analyses of fuel-rods. In addition to the influence of the gap size, end-pellets boundary conditions and the presence of the plenum spring with a pre-stressing force affects the contribution of the pellets to the overall bending stiffness of the fuel-rod. It is worth noting that this conclusion might change when irradiated fuel-rods are tested given that bonding between the pellets and the cladding may not be negligible, and the preload is reduced due to relaxation of the plenum spring. In addition, results might change if different gap sizes are present between cladding and pellets.

It was also shown that fuel-rod modal frequencies are very sensitive to changes in the degree of rotational restraint present at one or more support points. This implies that potential damages or changes to spacer grid springs, in addition to material degradation of the cladding, could make a fuel-rod more vulnerable to vibration-induced damage during normal conditions of transport. In this study, the first mode natural frequency varied from 7 to 36 Hz for different support point configurations for a Zr-4 fuel-rod with surrogate steel pellets with a total length that is about 50% of the active length of a rod in a WE 17 × 17 OFA assembly

This study presented a relatively simple approach that proved to be successful in calibrating numerical models of intact fuel-rods based on modal testing. To account for the rotational restraint of the end-supports, these were modelled as a combination of rotational springs and pin supports. This work represents a baseline for further experimental and numerical investigation on the mechanical performance of spent nuclear fuel-rods during normal conditions of transportation.

ACKNOWLEDGEMENTS

This material is based upon work supported under a Department of Energy Nuclear Energy University Programs (DE-NE0000698 001). Any opinions, findings, conclusions or recommendations expressed in this publication are those of the authors and do not necessarily reflect the views of the Department of Energy. The authors would like to provide special thanks to the consultant of this project, Justin Coleman, from Idaho National Laboratory for providing the Zircaloy fuel-rod.

REFERENCES

- ABAQUS (2013). Version 6.13, Dassault Systèmes Corp
- Adkins, H., Geelhood, K., Koeppel, B., Coleman, J., Bignell, J., Flores, G., Wang, J., Sanborn, S., Spears, S. and Klymyshyn, N., (2013). "Used Nuclear Fuel Loading and Structural Performance Under Normal Conditions of Transport-Demonstration of Approach and Results on Used Fuel Performance Characterization", September 30, *FCRD-UFD-2013-000325*, Pacific Northwest National Laboratory, Richland, WA.
- Klymyshyn, N. A., Sanborn, S. E., Adkins, H., and Hanson, B, D.,(2013). "Fuel Assembly Shaker Test Simulation.", May 30, *FCRD-UFD-2013-000168*, Pacific Northwest National Labrotary, Richland, WA.
- Copper-Tube (2015). "<http://www.mcmaster.com/#8965k27/=wt395t>."
- DOE/RW-0184 (1987). "High-level waste, and other radioactive wastes which may require long-term isolation. Office of civilian radioactive waste management", U.S. Department of Energy, Appendix 2A, Volume 3 of 6.
- Matweb(2015). "<http://www.matweb.com/search/DataSheet.aspx?MatGUID=a265da2e4ff94c968a8ae344870a32e3&ckck=1>, ATI Wah Chang."
- Steel-Rod (2015). "<http://www.mcmaster.com/#8890k259/=wt39jn>."
- NWTRB (2010) "Evaluation of the Technical Basis for Extended Dry Storage and Transportation of Used Nuclear Fuel.", Nuclear Waste Technical Review Board, December.